Mathematical modeling of kinetic oscillations in the catalytic CO oxidation on Pd(110): The subsurface oxygen model

Cite as: J. Chem. Phys. **93**, 811 (1990); https://doi.org/10.1063/1.459451
Submitted: 06 February 1990 . Accepted: 15 March 1990 . Published Online: 04 June 1998

M. R. Bassett, and R. Imbihl

Mathematical modeling of kinetic oscillations in the catalytic CO oxidation on Pd(110): The subsurface oxygen model

M. R. Bassett[a] and R. Imbihl
Fritz-Haber-Institut der Max-Planck-Gesellschaft, Faradayweg 4-6, D-1000 Berlin 33, Federal Republic of Germany

(Received 6 February 1990; accepted 15 March 1990)

Experimental investigations of the catalytic CO oxidation on a Pd(110) surface revealed that the temporal oscillations in the reaction rate (measured in a range 10^{-3} Torr $< p <$ 1 Torr) can be traced back to a periodic formation and depletion of oxygen in the subsurface region. Oscillations in the reaction rate arise because the variation in the subsurface oxygen concentration modulates the oxygen sticking coefficient and hence the catalytic activity. Based on the proposed reaction mechanism, which has been well supported by experimental data, a set of three coupled differential equations was established describing the variations in the absorbate coverages Θ_O and Θ_{CO} and in the subsurface oxygen concentration for the system Pd(110)/CO + O_2. Numerical solutions from the mathematical model reproduce the essential qualitative and quantitative features of the experiment. Characteristic features in the experiment that indicate the presence of subsurface oxygen, such as a reversal of the usual clockwise hysteresis in the reaction rate, are also found in the simulation. The model reproduces the existence region for kinetic oscillations in good agreement with the experimental data and it exhibits similar bifurcation behavior to that observed in the experiment. The remaining, mainly quantitative, differences can be traced back to simplifications made in the formulation of the kinetics.

I. INTRODUCTION

Kinetic oscillations in the catalytic CO oxidation have been studied both under low ($p < 1$ Torr) and high pressure conditions ($p > 1$ Torr) with various forms of Pd, Pt, and Ir catalysts.[1-3] Depending on the pressure range, and on the substrate, the proposed mechanisms can be separated into two groups. Experiments with Pt single crystal surfaces of (100), (110), and (210) orientation in the 10^{-5} and 10^{-4} Torr range revealed the existence of a common principle. The oscillations in the reaction rate are caused by periodic structural changes of the surface which modulate the oxygen sticking coefficient and hence the catalytic activity.[2,3] The mechanisms discussed for the high pressure oscillations are based on a different principle. The periodic change in the catalytic activity has been attributed to either a periodic oxidation and reduction of the Pt surface in the so-called oxide model[4] or alternatively to a periodic site blocking by carbon in the so-called carbon model.[5] The existence of two different groups of mechanisms can be traced back to the different conditions under which the oscillations occur. High pressure oscillations take place under nonisothermal conditions on contaminated surfaces thus facilitating oxide formation, while the formation of oxide or a carbon layer can be excluded in the Pt single crystals studies due to strictly isothermal conditions and contaminant-free surfaces.

A link between the high and low pressure experiments was established in a recent study where kinetic oscillations on a Pd(110) surface were investigated in an intermediate pressure regime between 10^{-3} and 1 Torr.[6-8] Different from Pt surfaces, clean Pd surfaces do not reconstruct, but the modulation of the catalytic activity of Pd(110) has been shown to be due to a periodic formation and depletion of oxygen in the subsurface region.[7] Although this mechanism resembles the oxide model suggested by Turner *et al.*,[4] an important difference exists since the subsurface oxygen species is different in nature from a real oxide. Subsurface oxygen can be reversibly converted into the reactive surface species, while an oxide of Pt or Pd is several orders of magnitude more unreactive towards CO and exhibits a much higher thermal stability.[9]

In this report we describe a mathematical model for the simulation of kinetic oscillations in the system Pd(110)/CO + O_2. The model is based on a periodic modulation of the catalytic activity of Pd(110) by the formation and removal of subsurface oxygen. The decisive role of subsurface oxygen in the mechanism of kinetic oscillations on Pd(110) has been verified in a number of detailed experiments.[7] Different from the oxide model,[4] which so far could not be verified by *in situ* experiments, the individual steps underlying the model used here are well supported by experimental observations and the results of the simulation can be compared with a wide set of experimental data. The results of the numerical simulation demonstrate that the subsurface oxygen model can in fact explain the kinetic oscillations on Pd(110) qualitatively and quantitatively well, while the remaining differences can be attributed to simplifications made in the model.

II. THE SURFACE MODEL

The model of catalytic CO oxidation on Pd(110) is based on the Langmuir–Hinshelwood (LH) mechanism

[a] Present address: Union Carbide Corporation, P.O. Box 8361, South Charleston, WV 25303.

 0021-9606/90/130811-11$03.00

which has to be modified to include the reversible formation of subsurface oxygen and its influence on the adsorption steps. The LH mechanism proceeds along the following sequence:[10]

$$CO + * \leftrightarrows CO_{ad},$$

$$O_2 + 2* \Rightarrow 2O_{ad},$$

$$O_{ad} + CO_{ad} \Rightarrow CO_2 + 2*$$

(* denotes a free adsorption site)

to which the reversible conversion of chemisorbed oxygen O_{ad} into subsurface oxygen O_{sub} has to be added,

$$O_{ad} \leftrightarrows O_{sub}.$$

The system Pd(110)/O_2 has been the subject of a number of studies focusing mainly on the adsorption/desorption kinetics and the formation of ordered adsorbate phases.[11-17] The energy diagram describing the penetration of adsorbed oxygen into the bulk region is depicted in Fig. 1. Here it has been assumed that the sites directly underneath the surface are energetically favorable compared to bulk sites and therefore are populated preferentially as soon as oxygen penetrates into the bulk region. We assume, as formulated above, that an equilibrium exists between adsorbed oxygen and oxygen on subsurface sites, while sites deeper inside the bulk are not populated substantially. This is of course a strong simplification since the energy difference between subsurface and bulk sites has not been determined experimentally and may in fact be very small. But this effect is considered to be of minor importance, since the occupation of deeper layers will not lead to a qualitatively different behavior of the model.

The energetic interaction between adsorbed oxygen atoms leads to a decrease in the adsorption energy E_{ad} of oxygen at higher coverages shifting the isosteric heat of adsorption from 80 kcal/mol in the limit of zero coverage to 48 kcal/mol at high oxygen coverages.[11] As indicated in Fig. 1

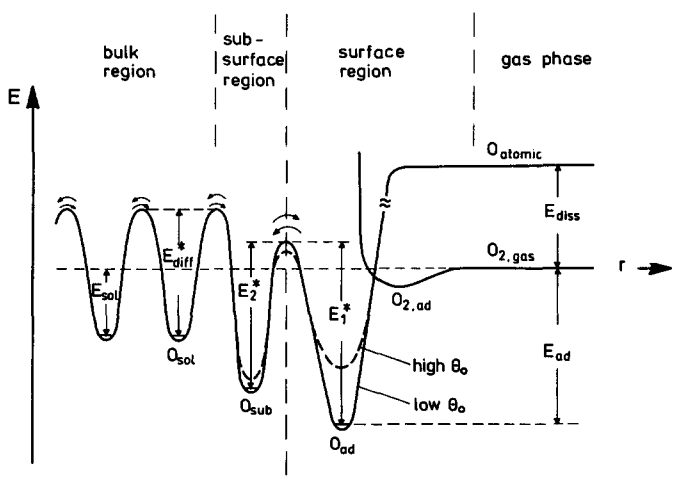

FIG. 1. Schematic energy diagram for the dissociative adsorption of oxygen and the incorporation of adsorbed atomic oxygen into the bulk of a Pd catalyst. O_{ad} and O_{sub} denote adsorbed atomic oxygen and oxygen underneath the top layer of the Pd substrate, respectively, while O_{sol} stands for oxygen dissolved in the deeper layers of the metal substrate. The activation energies E^*_1 and E^*_2 which control the reversible formation and removal of subsurface oxygen appear as the constants E^*_6 and E^*_7 in the mathematical model (see Table I).

the decrease in E_{ad} with increasing oxygen coverage may lead to a lowering of the energy barrier for the bulk penetration of oxygen. Thus, one can explain the experimental finding that noticeable formation of subsurface oxygen occurs only if the oxygen coverage Θ_O exceeds 0.5 corresponding to a $c(4\times2)$ pattern in LEED.[7,15] The effect of a coverage dependent activation energy for the penetration of oxygen has been neglected in our model, however, in order to keep the model as simple as possible. Calculations which included this effect showed only minor differences compared to the simpler model.

The strong influence of subsurface oxygen on the kinetics of catalytic CO oxidation on Pd(110) has been demonstrated experimentally very clearly, since the presence of this species caused a reversal of the usual clockwise hysteresis in the reaction rate (as p_{CO} is varied) into a counterclockwise hysteresis.[7] The change in the catalytic activity due to the presence of subsurface oxygen can be traced back to modification of the adsorption properties via a change in the electronic structure of the Pd(110) surface. Experimentally it has been demonstrated that subsurface oxygen causes a lowering of the adsorption energy of CO and a strong reduction of the oxygen sticking coefficient can be concluded from the sharp drop of the oxygen sticking coefficient beyond $\Theta_O = 0.5$, where subsurface sites start being populated.[7,15] Under oscillation conditions, which are at relatively low temperature ($\sim$400 K), only the latter effect will be of importance since oxygen adsorption is rate limiting for CO oxidation under these conditions.

One arrives at a set of three coupled differential equations (DE) describing the variations in the adsorbate coverages Θ_O and Θ_{CO} of oxygen and CO and the variation of the subsurface oxygen concentration c. Since we assume that the number of surface sites is equal to the number of subsurface sites, Θ_O, Θ_{CO}, and c all vary between 0 and 1 with $0 \leqslant c$, Θ_{CO}, and $\Theta_O \leqslant 1$:

$$\frac{d\Theta_{CO}}{dt} = K_1 p_{CO}(1-\Theta_{CO}) - K_2\Theta_{CO} - K_3\Theta_{CO}\Theta_O, \quad (1)$$

$$\frac{d\Theta_O}{dt} = K_4 p_{O_2} \exp(-K_5 c)(1-\Theta_{CO}-\Theta_O)^2 - K_3\Theta_{CO}\Theta_O - K_6\Theta_O(1-c) + K_7 c(1-\Theta_O), \quad (2)$$

$$\frac{dc}{dt} = K_6\Theta_O(1-c) - K_7 c(1-\Theta_O). \quad (3)$$

Simple Langmuir kinetics have been assumed for the adsorption of CO and oxygen taking into account that CO can still adsorb and react even on an oxygen saturated surface.[18-20] The treatment of the surface reaction between adsorbed CO and oxygen in the term containing K_3 neglects island formation. Equation (3) describes the diffusion processes of subsurface oxygen. Adsorbed oxygen penetrates into subsurface sites and the reverse process takes place as subsurface oxygen segregates back to the surface. The diffusion rate is set proportional to the concentration of the diffusing species and to the number of oxygen free sites to which the particles can diffuse. The presence of subsurface oxygen causes a decrease of the adsorption rate of oxygen. This is incorporated

in the term containing K_5 where an exponential dependence of the oxygen sticking coefficient on the subsurface oxygen concentration has been assumed. In an alternative formulation, the exponential dependence of s_{O_2} on the subsurface oxygen concentration was replaced by a linear relationship. This, however, yielded inferior quantitative agreement with the experimental results.

Kinetic oscillations take place in the model under isothermal conditions, at constant partial pressure, and on a spatially homogeneous Pd(110) surface. The isothermality of the reaction should be well fulfilled below $p = 1$ Torr, since the high thermal conductivity of a massive Pd single crystal, and the small heat production by the surface reaction, can hardly result in temperature changes of more than 0.1 K during kinetic oscillations. Depending on the pumping rate in the reaction chamber partial pressure variations up to a few percent have been observed experimentally as a consequence of mass balance in the reaction.[6-8] Since the model proved to be relatively insensitive to small variations in p_{CO} and p_{O_2}, however, the partial pressures were treated as being constant. Different from kinetic oscillations on Pt(100) where the structural transformations propagated wave-like across the surface, spatial synchronization on Pd(110) appears to be dominated by gas phase coupling.[8] This leads to a surface which oscillates homogeneously on a macroscopic scale similar to kinetic oscillations on Pt(110).[3]

Table I gives a listing of all constants used in the numerical simulation. These were derived as much as possible from experimental data published in the literature. Similar to oxygen, the adsorption behavior of CO on Pd(110) has also been investigated in great detail in a number of single crystal studies.[21,22] The surface reaction, which exhibits similar properties on all Pt and Pd surfaces, has been the subject of many studies,[10,18-20] but very few data are available about the kinetics of subsurface oxygen formation on Pd(110).[7,15] The adsorption constants k_1 and k_4 for CO and O_2 are expressed in monolayers (ML) per second. The initial sticking coefficient s_i^0 is included in the constants k_1 and k_4 according to

$$k_i = \lambda_i \cdot s_i^0 \cdot A_i \quad \text{for } i = 1,4,$$

where

$A_i = 1$ for associative adsorption,

$A_i = 2$ for dissociative adsorption,

and where λ_i denotes the impingement rate of the gas particles from kinetic gas theory. Experimentally $s_{CO}^0 = 1$ has been determined for CO adsorption and $s_{O_2}^0 = 0.86$ for oxygen adsorption on Pd(110).[12,22]

CO TD spectra of Pd(110) revealed the existence of three distinct adsorption states.[21] Since the oscillations occur at relatively low temperature around ~400 K under conditions of a high CO coverage, the adsorption energy of the high coverage α state ($E_{ad} = 24$ kcal/mol with a peak temperature of 330 K in TDS) was used for the simulation. In a detailed titration study of the catalytic CO oxidation on Pd(110) it has been demonstrated that the kinetic parameters of the surface reaction depend very strongly on the oxygen coverage.[19] The compensation effect between an increase of the activation energy and a concomitant increase of the frequency factor, however, makes the actual reaction rate almost independent of the oxygen coverage over a wide coverage range. This effect justifies the simpler approach of using coverage independent parameters. For the simulation the kinetic parameters of the LH reaction were not taken from the titration study but from a molecular beam study of the catalytic CO oxidation on Pd(111), where steady-state conditions had been used.[20] In this study the activation energy of the reaction has also been shown to be strongly dependent on the coverage and decreases from 25 kcal/mol at low coverage to 14 kcal/mol at higher coverages.[20] For the kinetic parameters of the diffusion of subsurface oxygen estimates had to be made using an activation energy $E^* = 20$ kcal/mol for the bulk diffusion of oxygen in Pd as a guideline.[23] Since the time scale of the segregation of subsurface oxygen is known experimentally to be in the order of several minutes at 400 K,[7] the kinetics of this process can be approximated quite well in the narrow temperature window where oscillations occur.

The assumption of simple adsorption kinetics of the Langmuirian type for CO and O_2 on Pd(110) is a rather gross simplification, since it is well known that both gases obey precursor kinetics in their adsorption behavior on this surface.[12,21,22] Besides the simplified version of the model, therefore, a more realistic version including precursor kinetics for CO and O_2 adsorption was also investigated. Since precursor kinetics for CO adsorption affected the behavior of the oscillations only to a small extent, the original simple version used in Eq. (1) was kept for CO adsorption. Precursor kinetics for O_2 adsorption also did not change the qualitative behavior of the model appreciably. They proved, however, to be indispensible in order to obtain a quantitative fit to the experimental data. All diagrams presented in this paper were accordingly calculated using the "realistic" version of the model with precursor kinetics for O_2 adsorption as follows.

Precursor kinetics for dissociative adsorption can be formulated according to Kisliuk[24] as

$$s(\vartheta)/s^0 = \frac{(1-\vartheta)^2}{1-\vartheta(1-K)+\vartheta^2 s^0},$$

where ϑ denotes the relative coverage and the parameter K determines the influence of the precursor state. Figure 2 shows that the experimentally determined curve for O_2 adsorption at $T = 354$ K can be well approximated with the expression derived by Kisliuk using $K = -0.90$ as a parameter. Since a precursor for O_2 adsorption will probably not exist on the CO covered surface, the parameter K which determines the influence of the precursor state has been made coverage dependent with $K = -0.9 + 1.9\,\Theta_{CO}$. The O_2 adsorption kinetics then change continuously with the CO coverage such that the influence of the precursor is no longer present for a completely CO covered surface with K being equal to 1. This is shown in Fig. 2. In the realistic version of the model Eq. (2) then reads

TABLE I. Constants used in the mathematical model with $k_i = \nu_i \exp(-E_i^*/RT)$.

Description	Constant	E_i^*(kcal/mol)	ν_i(s^{-1})	Value for 400 K[a]	References
CO adsorption	k_1	...	...	4.1×10^5 ML s^{-1} $Torr^{-1}$	21 and 22
CO desorption	k_2	24	4.35×10^{13}	$3.0\ s^{-1}$	21 and 22
Surface reaction	k_3	14	8.6×10^9	$1.8\times10^2\ s^{-1}$	20[b]
O_2 adsorption	k_4	...	...	7.6×10^5 ML s^{-1} $Torr^{-1}$	12
O_{sub} influence on O_2 adsorption	k_5	...	...	10	fit parameter
O diffusion surface bulk	k_6	10	3.0×10^4	$9.8\times10^{-2}\ s^{-1}$	estimate
O diffusion bulk surface	k_7	28	2.5×10^{12}	$1.1\times10^{-3}\ s^{-1}$	estimate
Parameter precursor kinetics	k_8	...	...	-0.95	...

[a]ML = monolayer.
[b]In the simulation ν_3 was increased by a factor of 100 compared to the value given in Ref. 20.

$$\frac{d\Theta_O}{dt} = k_4 p_{O_2} \exp(-K_5 c) \times\left(\frac{(1-\vartheta)^2}{1-\vartheta(1-k_8-1.9\Theta_{CO})+\vartheta^2}\right) - K_3\Theta_O\Theta_{CO} - K_6\Theta_O(1-c) + K_7 c(1-\Theta_O) \quad (2')$$

with $\vartheta = \Theta_O + \Theta_{CO}$.

III. RESULTS

A. Mechanism of kinetic oscillations

The occurrence of kinetic oscillations is restricted to a certain p_{O_2}, p_{CO}, T-parameter range which experimentally is usually determined by varying one of the parameters over a wide range while the other two are held constant. Figure 3 shows the variation of the reaction rate r_{CO_2} in the numerical simulation as p_{CO} was slowly varied in a cycle, while the temperature and p_{O_2} were kept constant at $T = 420$ K and $p_{O_2} = 4\times10^{-2}$ Torr. Kinetic oscillations develop during the backward scan in a broad region around the rate maximum which separates the low p_{CO} region where the surface is predominantly oxygen covered from the high p_{CO} region where the surface is predominantly CO covered. The hysteresis in the reaction rate exhibits a remarkable feature in that its sense of rotation has been reversed compared to the usual clockwise hysteresis observed in the catalytic CO oxidation on Pt surfaces. The reversal of the hysteresis reflects the influence of subsurface oxygen on the catalytic activity and originates from the filling of the subsurface oxygen reservoir at low p_{CO} and its depletion at high p_{CO}. The apparent hysteresis in Fig. 3 is not a real hysteresis since, as will be shown below, it does not correspond to an actual bistability in the rate of CO_2 production but is due to kinetic effects as the formation and removal of subsurface oxygen proceed on a very slow time scale.

The comparison of the calculated hysteresis with the experimental one obtained by Ladas *et al.*[7] demonstrates excellent agreement in the behavior of the reaction rate and

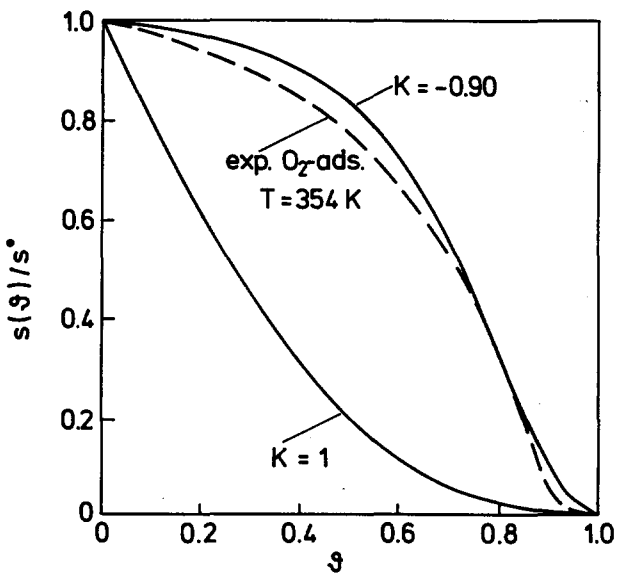

FIG. 2. Comparison between the experimentally determined coverage dependence of s_{O_2} for Pd(110) (Refs 12 and 22) and the calculated variation of $s_{O_2}(\vartheta)$ using the Kisliuk model with $K = -0.90$ (see the text). In order to convert the experimental $s(\Theta)$ curve into a $s(\vartheta)$ curve via $s(\vartheta) = s(\theta)/\theta_{sat}$, a nominal saturation coverage $\Theta_{sat} = 0.55$ has been assumed. The curve calculated with $K = 1$ is meant to represent O_2 adsorption on a surface where a precursor state is no longer present.

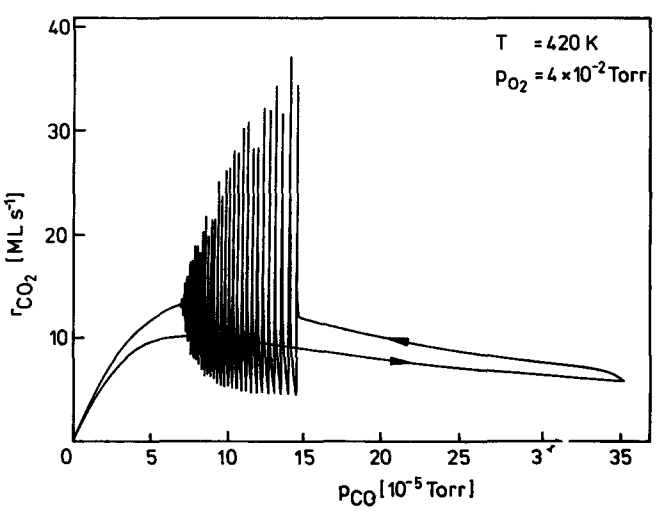

FIG. 3. Calculated variations in the reaction rate as p_{CO} is slowly varied in a cycle using a linear ramp for p_{CO} and a sweep rate of 1.5×10^{-7} Torr/s.

in the position and width of the existence region for oscillations. Oscillations were found to occur in the vicinity of the rate maximum at a large partial pressure ratio p_{O_2}/p_{CO} in the order of 100:1 to 1000:1, and at relatively low temperature in the range from ~ 350 to ~ 450 K.[6-8] An example of the relaxation-type oscillations obtained at the position of the rate maximum in Fig. 3 is displayed in Fig. 4. The individual steps of the mechanism for kinetic oscillations, as deduced from the variation of the three variables Θ_O, Θ_{CO}, and c in Fig. 4, can be formulated as follows:

(1) Starting with a CO covered surface the subsurface oxygen reservoir is slowly depleted as subsurface oxygen segregates to the surface and reacts off with adsorbed CO. The decrease in subsurface oxygen concentration leads to a concomitant increase in s_{O_2} and consequently one observes a continuous decrease of the "steady-state" concentration of adsorbed CO. Since adsorbed CO inhibits the adsorption of oxygen the rate of CO_2 production will be low in this part of the period of oscillation where the surface is predominantly covered by CO.

(2) At some point oxygen adsorption will become dominating in comparison with CO adsorption. In a rather sudden transition the state switches from a predominantly CO covered surface to a surface with a high concentration of oxygen on it. This transition is associated with a sharp increase of the reaction rate, as the reaction rate is proportional to the oxygen coverage Θ_O.

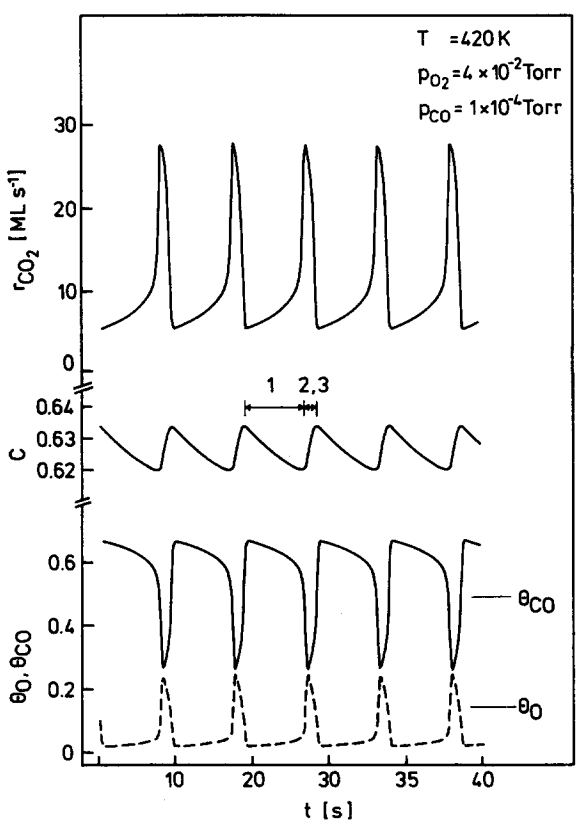

FIG. 4. Calculated variation of the reaction rate r_{CO_2}, the adsorbate coverages Θ_O and Θ_{CO}, and the subsurface oxygen concentration c during kinetic oscillations on Pd(110). The p_{O_2}, T conditions correspond to those of the r_{CO_2} vs p_{CO} diagram displayed in Fig. 3.

(3) With the oxygen coverage being high, the refilling of the subsurface oxygen reservoir begins. Consequently s_{O_2} will decrease and at some point CO adsorption will again dominate over oxygen adsorption leading back to the initial situation of a CO covered surface.

The mechanism presented here is identical to that proposed in the experimental paper by Ladas *et al.*[7] The essential part of the mechanism is the reversible formation of subsurface oxygen whose equilibrium concentration is solely determined by the oxygen coverage (at constant T). The necessary feedback behavior for oscillations is accomplished via the change in the oxygen sticking coefficient which becomes smaller as the concentration of subsurface oxygen increases. Due to the strong dependence of s_{O_2} on c, as given by the large value of $K_5 = 10$, the large variations in the reaction rate are accompanied by only small variations in c, of the order of $\sim 1\%$ at 420 K. At lower temperature the variations Δc become larger and reach an amplitude of $\sim 10\%$ at 390 K. The smallness of Δc might be unrealistic since it originates mainly from using K_5 as the main fit parameter for adjusting the existence region of the simulated oscillations to the experimental data. In the relaxation-type oscillations displayed in Fig. 4, the period is determined by the slow segregation of oxygen to the surface. The period of ~ 10 s agrees with the experimentally determined period of oscillations in the 10^{-2} Torr range at ~ 400 K.[6,8]

B. The existence region for oscillations

The existence region for kinetic oscillations has been mapped out for various p_{CO}, p_{O_2}, T conditions which are represented in the Arrhenius plot of $\ln p_{CO}$ vs $1/T$ in Fig. 5(a) as lines of constant p_{O_2}. The data points used in this figure marking the center of the oscillation region were obtained by taking the average of the upper and lower p_{CO} limit for oscillations at a given temperature and p_{O_2}. The same representation of the data has been used presenting the experimental results[6] in Fig. 5(b) and the results can therefore be compared directly. The comparison shows that quite a number of the experimentally observed features are reproduced well by the model.

First, an upper temperature limit for oscillations exists whose dependence on the T, p_{O_2}, p_{CO} conditions can be represented by the dashed straight line in Fig. 5(a). The slope of this line corresponds to an "activation" energy of 26 kcal/mol in reasonable good agreement with the experimental value of 22 ± 2 kcal/mol.[6]

Second, the p_{O_2} isobaric lines in Fig. 5(a) all yield the same apparent activation energy of 19 kcal/mol. This value is too high when compared to the experimental value of 11 kcal/mol.[6] Apparently in this range the model does not work quantitatively as well as it does in the boundary region of the oscillations.

Third, the oscillating conditions at constant temperature follow the relationship

$$p_{CO} \sim \sqrt{p_{O_2}}.$$

This relationship has also been found in the experiment.[6,7] Since the center of the oscillation region coincides approxi-

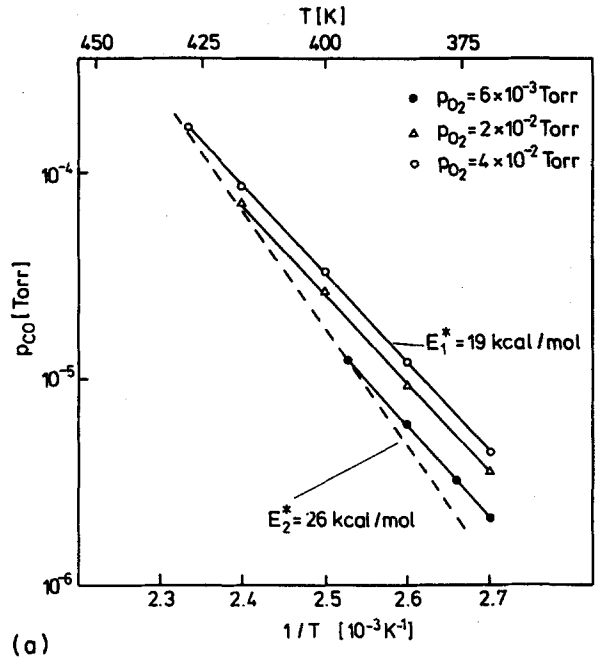

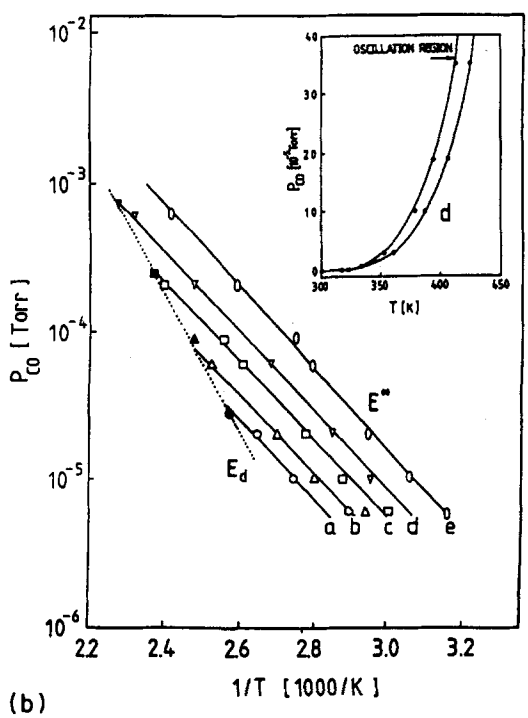

FIG. 5. (a) Calculated existence diagram for kinetic oscillations in the system Pd(110)/CO + O_2. The p_{CO}, T conditions for kinetic oscillations have been mapped for three different p_{O_2} represented by different symbols in the plot. (b) Experimentally determined existence diagram for kinetic oscillations on Pd(110) obtained by Ehsasi *et al.* (Ref. 6). The existence region represented by p_{O_2} isobaric lines is shown for four different p_{O_2}: (a) 6.0×10^{-3} Torr; (b) 1.0×10^{-2} Torr; (c) 2.0×10^{-2} Torr; (d) 4.0×10^{-2} Torr; (e) 1.0×10^{-1} Torr. The full lines all represent the same activation energy of 11 ± 1 kcal/mol, while the dotted line yields an activation energy of 22 ± 1.5 kcal/mol. The inset displays the oscillation region in the p_{CO}, T-parameter plane for a fixed $p_{O_2}=4.0\times10^{-2}$ Torr. (Reproduced with permission of the authors.)

mately with the position of the rate maximum in a r_{CO_2} vs p_{CO} plot (see Fig. 3), the above relationship can be deduced very simply using Langmuirian kinetics and the assumption that both gases compete for the same (small) number of free sites. The square root dependence is then determined by the fact that an oxygen molecule, when dissociating, needs two free sites for adsorption as compared to CO for which a single free site suffices.

In order to achieve reasonable quantitative agreement between the calculated and the experimental existence region for oscillations precursor kinetics for O_2 adsorption proved to be an indispensable part of the simulation. These had mainly the effect of shifting the whole calculated existence region towards higher temperature. The discrepancy between the actual and the calculated p_{CO} values which differ in a wide T- range by up to a factor of 5, can largely be traced back to neglecting the influence of adsorbed oxygen on the adsorption kinetics of CO in Eq. (1). Experimentally it has been shown that preadsorbed oxygen on Pd(110) can reduce s_{CO} up to a factor of 2.[18] This had to be compensated for in the calculation by a corresponding increase in p_{CO}.

The two different slopes which exist in the Arrhenius diagram in Fig. 5(a) cannot be assigned to an activation energy of one of the elementary steps listed in Table I, although the near coincidence of the adsorption energy of CO, $E_2^* = 24$ kcal/mol, with the apparent activation energy of 26 kcal/mol of the high-T boundary in Fig. 5(a) suggests such a relationship. The simulation showed, however, that this slope depends very strongly on K_5 and can even change sign with appropriate constants. Therefore, in the simulation at least a definite connection between the α state for CO adsorption and the high-T boundary for kinetic oscillations on Pd(110) does not exist. The interpretation of the second activation energy of 19 kcal/mol corresponding to the slope of the p_{O_2} isobars in Fig. 5(a) is simpler. Under conditions where the surface reaction and not the adsorption of oxygen is rate limiting for the CO_2 production, the slope of the p_{O_2} isobars becomes equal to the activation energy of the surface reaction. These conditions are not fulfilled in the present case and the value of 19 kcal/mol determined in the simulation is therefore somewhat higher than the activation energy, $E_3^* = 14$ kcal/mol, for the surface reaction.

Using AUTO, a published program package which contains continuation algorithms for constructing bifurcation diagrams,[25] the existence region of the oscillations at constant p_{O_2} has been determined in the p_{CO}, T parameter plane. This is shown in Fig. 6. The same diagram has also been determined experimentally for $p_{O_2}=4\times10^{-2}$ Torr by Ehsasi *et al.*,[6] and therefore a direct comparison between theory and experiment can once again be made. If one compares the calculated existence region with the experimentally determined region displayed in the insert of Fig. 5(b), one notices that both plots exhibit the same qualitative behavior with an existence region which shifts up exponentially in p_{CO} with increasing temperature. Below 350 K the existence range basically shrinks to zero both in the experimental results and in the simulated oscillations. The temperature range in which oscillations can be obtained extends from

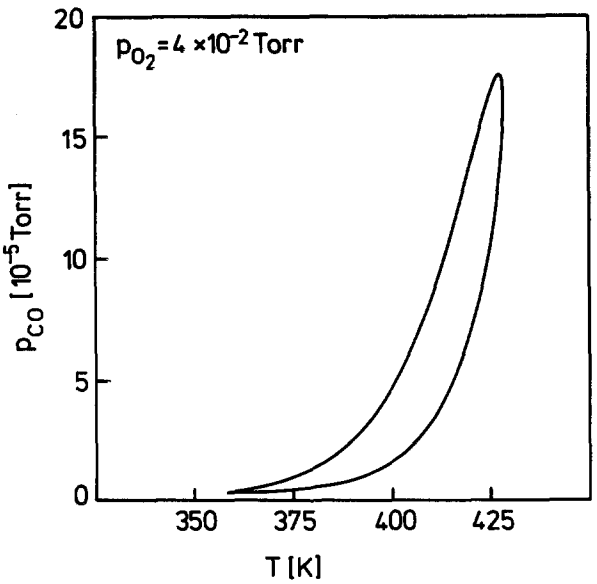

FIG. 6. Calculated existence region for kinetic oscillations in the p_{CO}, T-parameter plane for a fixed $p_{O_2} = 4 \times 10^{-2}$ Torr.

~350 K to ~425 K in both plots. The exponential increase in p_{CO} with rising temperature corresponds to an activation energy of 24 kcal/mol in the calculated diagram. Since this value is identical to the adsorption energy E_2^* of the α state of adsorbed CO, the high coverage state of adsorbed CO is apparently the important one in the mechanism of the oscillations. The width of the oscillatory temperature region for a given p_{CO} extends over 10 to 15 K in the simulated as well as in the experimental diagram. For reasons discussed above, the p_{CO} values in the calculated existence region are too low by roughly a factor of 5, but otherwise the agreement between theory and experiment is excellent. An additional important feature not contained in the experimentally determined existence region is that the calculated diagram exhibits an upper p_{CO} limit for oscillations (for a given p_{O_2}). The calculated existence range is therefore represented by a closed curve, while the experimental range is open towards higher p_{CO}. This discrepancy is very clearly due to the fact that too small of a parameter range was investigated experimentally since a given p_{O_2} value will always impose a certain upper p_{CO} limit for obtaining oscillations.

C. Bifurcation behavior

Figure 3 reveals the existence of two qualitatively different kinds of transition to oscillatory behavior as p_{CO} is swept across the existence region for oscillations. At the low p_{CO} limit the amplitude of oscillations grows continuously as p_{CO} enters the oscillatory region, while the amplitude of the oscillations discontinuously jumps to zero in a sudden transition at the high p_{CO} limit. The qualitatively different behavior of the oscillations at the transition points corresponds mathematically to a different kind of branching of the solutions to the kinetic equations. The different branching mechanisms at the bifurcation points can be conveniently followed for a given set of DE's using the continuation algorithms in AUTO.

Using AUTO the steady-state diagram shown in Fig. 7(a) has been determined which corresponds directly to the simulated p_{CO} sweep displayed in Fig. 3. First, one notices that the system exhibits a single steady state whose stable steady-state regions are indicated by the full line in Fig. 7(a), while the dashed line represents an unstable steady state. The absence of multiple steady states demonstrates that the apparent hysteresis seen in Fig. 3 is not a true hysteresis, but results from kinetic effects, e.g., the slow segregation of subsurface oxygen. In other words, the hysteresis disappears if the ramping of p_{CO} is carried out sufficiently slowly.

As p_{CO} is increased past the low p_{CO} boundary the steady-state solution becomes unstable and a limit cycle is created surrounding the unstable steady state. This happens in a so-called supercritical Hopf bifurcation where the amplitude grows continuously as p_{CO} is increases past the bifurcation point. This can be seen very clearly in Fig. 7(a) where

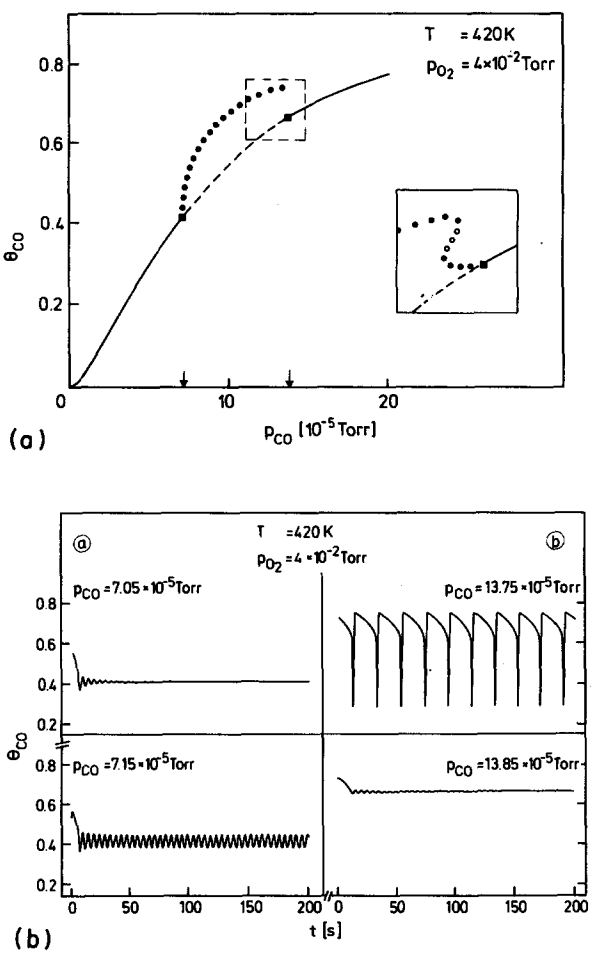

FIG. 7. (a) Bifurcation diagram for the system Pd(110)/CO + O_2 using p_{CO} as a bifurcation parameter, while the state of the system is represented by the CO coverage Θ_{CO}. Full lines indicate a stable steady state, dashed lines an unstable steady state. Hopf bifurcation points are marked by filled squares. Filled circles denote the upper limit of a stable limit cycle, while empty circles represent an unstable limit cycle. The inset shows in a schematic diagram a cyclic fold which presumably terminates the oscillatory region at the high p_{CO} boundary (see the text). (b) Examples of damped and sustained kinetic oscillations which can be obtained at various points of the bifurcation diagram displayed in (a).

filled circles mark the upper limit of the oscillation amplitude in the Θ_{CO}, p_{CO} plane. A supercritical Hopf bifurcation also exists at the upper p_{CO} boundary, but as p_{CO} is decreased only slightly below the bifurcation point the amplitude sharply increases to a large value leading to the seemingly discontinuous change of oscillation amplitude visible in Figs. 3 and 7(a). This behavior is very likely due to a second bifurcation past the primary Hopf bifurcation in which coexisting stable and unstable limit cycles coalesce in a so-called cyclic fold as indicated in the insert in Fig. 7(a). One cannot exclude the possibility that the sharp rise of the oscillation amplitude is not due to a cyclic fold, but proceeds in a continuous way as a result of the supercritical Hopf bifurcation. Although this possibility appears to be less likely, it has not been possible using AUTO to distinguish between the two alternatives.

Examples of the different types of kinetic oscillations which can be obtained at different points of the bifurcation diagram of Fig. 7(a) are displayed in Fig. 7(b). At $p_{CO} = 7.15\times10^{-5}$ Torr, which is just above the lower supercritical Hopf bifurcation, sinusoidal oscillations with small amplitude can be observed. With increasing p_{CO} the amplitude of the oscillations grows and the character changes from sinusoidal oscillations to oscillations of the relaxation type. An example of the latter type is displayed for $p_{CO} = 1.375\times10^{-4}$ Torr. At p_{CO} values that lie just below (above) the lower (upper) bifurcation the system relaxes to the stable steady state via damped oscillations. This behavior is due to the existence of a stable focus in the neighborhood of a Hopf bifurcation.

The experimentally observed behavior of the oscillations near the boundaries of the existence region agrees with the calculated bifurcation diagram since the two different types of transitions have also been found there.[6,8] The occurrence of sinusoidal oscillations close to the low p_{CO} boundary has also been found in the experiment. Other trends observed in the experiment were also reproduced by the simulation, as is illustrated by the examples displayed in Fig. 8. With increasing temperature the oscillations increase in frequency, but the amplitude decreases as demonstrated in Fig. 8(b). Increasing the total pressure also causes an increase in the oscillation frequency as shown in Fig. 8(a).

A very peculiar bifurcation behavior has been observed by Ehsasi[8] at very low temperatures ($T\sim350$ K and $p_{O_2} = 4.5\times10^{-2}$ Torr) just at the boundary of the existence region for oscillations in Fig. 6. A very slight variation in the parameters—e.g., a temperature change from 352.6 to 353.9 K or a p_{CO} change by less than 1%—is sufficient to induce a change from oscillation which occur near the $\Delta\Phi$ level of the oxygen covered surface to oscillations which occur on a predominantly CO-covered surface. Induced by a small parameter change the reaction switches between two different oscillatory regions that are located around the two branches of the LH kinetics associated with an oxygen covered and a CO covered surface, respectively.

In the same parameter region where the observations described above were made, the steady-state solutions of the kinetic equations change from the monostable behavior shown in Fig. 7(a) to bistability. As will be shown below the

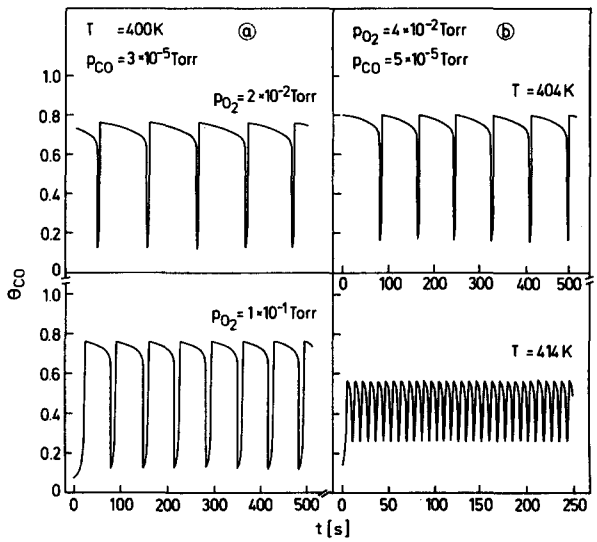

FIG. 8. Trends in the variation of the amplitude and frequency of kinetic oscillations for different parameter values of T, p_{CO}, and p_{O_2}.

increasing complexity of the bifurcation diagram and its sensitivity to small parameter changes is apparently related to the experimental observation of complex dynamical behavior in the same region. The bifurcation diagram of the corresponding parameter region at $T = 360$ K and $p_{O_2} = 4\times10^{-2}$ Torr is displayed in Fig. 9. Multiple steady states exist between ${}^{P}A$ and ${}^{P}C$. Two Hopf bifurcations, indicated by filled squares in Fig. 9, were detected at B and D. For p_{CO} between ${}^{P}A$ and ${}^{P}B$ one stable steady state exists coexisting with a saddle point and an unstable steady state. For p_{CO} values between ${}^{P}B$ and ${}^{P}C$, two unstable steady states and a saddle point are surrounded by a stable limit cycle. If p_{CO} is above ${}^{P}C$ and below ${}^{P}D$ another limit cycle exists located around the unstable steady state. The model predicts that small variations in p_{CO}, e.g., a change from 3.04×10^{-6} to 3.34×10^{-6} Torr, can cause the system to jump from an oxygen covered surface to a CO covered surface. This jump involves only a change from one steady state to another steady state, without oscillations occurring. Oscillations exist between ${}^{P}B$ and ${}^{P}D$, however, they are not restricted to either the upper or the lower branch, but encompass both branches. In this very narrow oscillating region the surface will therefore fluctuate between the oxygen covered and the CO covered state. An analogous bifurcation diagram to the one discussed above is obtained if one varies the temperature instead of p_{CO} as the bifurcation parameter. Figure 10 shows that a temperature change of 0.5 K is sufficient to cause the reaction to jump from a stable CO covered to a stable oxygen covered surface.

The simulation reproduces the high sensitivity of the system to small parameter changes. These small changes can easily make the reaction switch back and forth between the two branches of the LH kinetics due to the narrowness of the bistable region. The situation still does not correspond to the experimental one where the reaction switches between two different oscillating regions and not between two stable

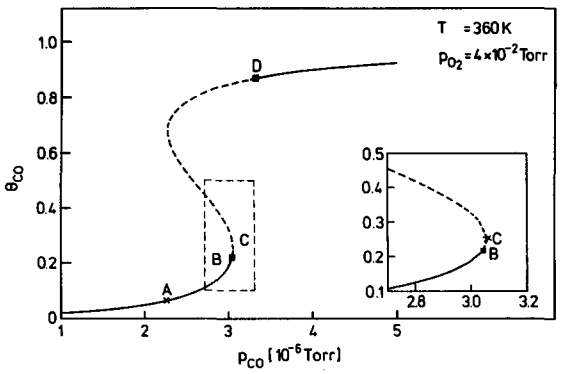

FIG. 9. Bifurcation diagram near the low T limit for kinetic oscillations (see Fig. 6) using p_{CO} as a bifurcation parameter. For an explanation of the different symbols used in the plot see the legend of Fig. 7(a).

steady states. However, since the system reacts very sensitive to parameter changes, it is very easy to imagine that any kind of additional feedback behavior is sufficient to provoke a more complex response of the system, i.e., that kinetic oscillations can also occur around each of the two branches. Additional feedback mechanisms which have not been included in the kinetic model could be provided by partial pressure variations accompanying the oscillations in the reaction rate, and by the possible influence of island formation and phase transitions within the chemisorbed layer. Interestingly, in the same parameter region where the bifurcation behavior becomes complex one observes chaotic oscillatory behavior and period doubling.[6] This coincidence suggests that the complexity of the dynamics is essentially caused by the sensitivity of the bifurcation behavior plus some additional feedback mechanism which remains to be identified.

IV. DISCUSSION

The results of the numerical simulation demonstrate that the subsurface oxygen model can reproduce almost all of the characteristic features of kinetic oscillations in the system Pd(110)/CO + O_2: the existence region, the bifurcation behavior, and most of the experimentally observed trends with respect to frequency and amplitude. Despite the good agreement between theory and experiment one has to keep in mind that successful mathematical modeling does not necessarily prove the correctness of the underlying physical assumptions. These have to be based on experimental verifications and alternative mechanisms should be considered as well. When the first considerations were undertaken to explain the experimental studies of this oscillating system the subsurface oxygen model appeared to be the only plausible mechanism for kinetic oscillations on Pd(110). The results of a recent reflection absorption infrared spectroscopy (RAIRS) study by Raval *et al.*,[29] however, has introduced a completely new aspect in terms of the proposed existence of a CO-induced reconstruction of the Pd(110) surface. Thus similar to Pt(110), the possibility of an oscillation mechanism based on an adsorbate-induced phase transition of the substrate comes into play. This possibility had been discarded before since the clean Pd(110) surface is nonreconstructed. In contrast to Pt(110) where CO lifts the reconstruction, CO on Pd(110) induces a reconstruction which exists at intermediate CO coverages between $\Theta_{CO} = 0.3$ and $\Theta_{CO} = 0.75$ according to the results of Raval *et al.* Similar to Pt(110), however, a 1×2 reconstruction of the "missing row" type has been proposed as a structural model for the reconstructed Pd(110) surface.[29]

Assuming that the two different substrate configurations of Pd(110) are associated with different catalytic activities, e.g., different oxygen sticking coefficients for example, kinetic oscillations on Pd(110) should be possible along the same mechanistic pathway via periodic structural changes that has been verified for Pt(100) and Pt(110).[2,3] Kinetic oscillations should then, however, also occur at pressures lower than 10^{-3} Torr. The phase transition model offers no plausible explanation for the existence of such a high low pressure limit for kinetic oscillations. Moreover, parallel measurements of LEED intensities and the kinetics of CO_2 production that were undertaken under stationary conditions in the 10^{-4} Torr range on Pd(110) did not reveal any kinetic instabilities whose existence could be related to the LEED structures associated with the proposed phase transition of the substrate.[30] A characteristic feature of the catalytic CO oxidation under oscillating conditions such as the reversal of the hysteresis in the reaction rate can consistently be explained by the subsurface oxygen model, while the phase transition model offers no simple interpretation of this effect. Thus, even in the light of the recent discovery that probably a CO-induced reconstruction exists on Pd(110), the subsurface oxygen model still appears to be valid for the mechanism of kinetic oscillations on Pd(110). It is quite evident that structural changes of the substrate via a CO-induced reconstruction will take place during kinetic oscillations on Pd(110). Their role in the oscillating mechanism is, however, not clear and at the present they appear to be of minor importance as compared to subsurface oxygen formation.

The most striking experimental difference between kinetic oscillations on Pd(110) and kinetic oscillations on Pt single crystal surfaces has been the existence of a low pressure limit of $\sim 10^{-3}$ Torr for Pd(110). Pt surfaces exhibited oscillatory behavior also at lower pressure in the 10^{-5} and 10^{-4} Torr range. This difference of roughly two orders of magnitude was taken as indirect evidence for the operation of a different oscillation mechanism on Pd(110) when compared to the surface phase transition mechanism on Pt surfaces. The reasons why no oscillations were detected on Pd(110) below 10^{-3} Torr can be seen from the existence diagram shown in Fig. 5(a). Extrapolating the upper temperature limit represented by the dashed line in Fig. 5 for $p_{O_2} = 1\times10^{-4}$ Torr yields a value close to 300 K. Due to some strongly activated steps in the mechanism the oscillation period becomes immeasurable long at this temperature thus excluding the observation of oscillations for practical reasons. Thus the low pressure limit of 10^{-3} Torr for kinetic oscillations on Pd(110) is not due to a real thermodynamical limit, but follows from the practical kinetics of the various processes involved. The range in which the subsurface oxygen model is applicable should also exhibit a high pressure limit. This is because oxide formation will set in at high-

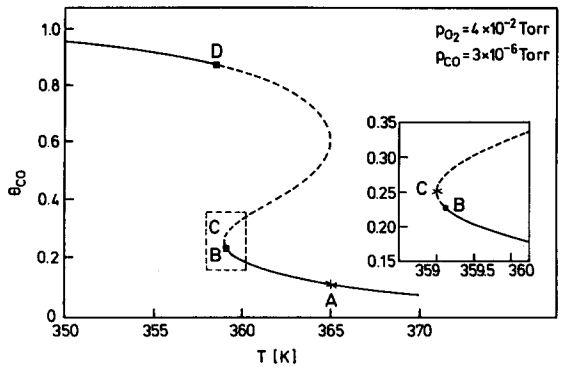

FIG. 10. Bifurcation diagram near the low T limit for kinetic oscillations (see Fig. 6) using the temperature T as a bifurcation parameter. For an explanation of the different symbols used in the plot see the legend of Fig. 7(a).

er p_{O_2} due to thermodynamical reasons. One would expect then a possible transition to a different oscillating mechanism based on the periodic oxidation and reduction of the surface as suggested by Turner *et al.*[4] This transition has so far not been investigated experimentally, as no oscillation experiments were undertaken in the pressure range between 1 Torr and 1 atm.

The comparison between the experimental and the calculated existence diagrams for kinetic oscillations did not resolve the question as to which process determines the high temperature boundary of the existence region for oscillations. In the experimental paper[6] the α state of adsorbed CO, whose adsorption energy of 24 kcal/mol agrees well with the activation energy of 22 ± 2 kcal/mol derived from the slope of the high T boundary was proposed as the state which determines the high T boundary. This assignment if correct would also have implications for the mechanism of kinetic oscillations on Pd(110). The unusual sharpness of the α state in TDS in which adsorbed CO desorbs between $\Theta_{CO} = 0.75$ and $\Theta_{CO} = 1.0$ has been associated by Raval *et al.*[29] with the CO-induced reconstruction of Pd(110) that was found to take place in the same coverage range. This assignment might however be based on the accidental coincidence of two activation energies as suggested by the simulation where the slope of the high T boundary was not determined by the adsorption energy of CO. The question as to whether the interpretation of the high T boundary in the experimental paper was incorrect or whether the kinetic model has to be improved to include the effect of the CO-induced reconstruction associated with the α state therefore remains open.

In order to improve the mathematical model it would be certainly desirable to have better experimental data on the kinetics of subsurface oxygen formation and its influence on the adsorption properties of Pd(110). These important relations are known more or less only qualitatively. The constant K_5 describing the influence of subsurface oxygen on O_2 adsorption therefore had to be treated as a mere fit parameter which introduces an uncertainty into the numerical simulation thereby diminishing the value of some of the quantitative results.

Despite these shortcomings the subsurface oxygen model presented here is one which comes close to a real quantitative description of kinetic oscillations in the catalytic CO oxidation. A detailed mathematical model that gives excellent qualitative results has been presented for the system Pt(100)/CO + O_2,[26,27] but due to the complexity of the system, which involves spatial pattern formation, the experimental as well as the theoretical characterization has been mostly qualitative. A three-variable model based on the $1\times1 \leftrightarrows 1\times2$ phase transition could reproduce many of the qualitative and quantitative features of kinetic oscillations on Pt(110).[28,31] Quite a number of models have been worked out to describe kinetic oscillations in the catalytic CO oxidation under high pressure conditions ($p > 1$ Torr).[1] Among these models the so-called oxide model has been widely accepted because oxide formation is known to occur at high pressure on Pt surfaces. These surfaces have normally not been made contaminant free by any special cleaning procedure.[35,36] Similar to our model the kinetic equations in the oxide model are based on the validity of the LH mechanism and involve two oxygen species with different reactivity towards CO.[4,36–38] The two models differ however with respect to the nature of the second, less reactive oxygen species and its influence on the LH kinetics. In the model presented here subsurface oxygen can be reversibly converted into chemisorbed oxygen, while oxide formation in the oxide model has been formulated as an irreversible step. The oxide then decreases the catalytic activity by blocking adsorption sites for CO and O_2, while in the subsurface oxygen model a lowering of the catalytic activity takes place via a decrease in the oxygen sticking coefficient. The different treatment of the second oxygen species in the two models is, however, due to the different behavior of Pt and Pd towards oxygen. The subsurface oxygen on Pd(110) and the oxide on Pt surfaces are two chemically different species with different geometric locations on the catalyst surface. However, the crucial point in a discussion of the oxide model is clearly the lack of an experimental verification of the proposed mechanism by *in situ* experiments. Measurements with Auger electron spectroscopy (AES) and Fourier transform infrared spectroscopy (FTIR) could not detect any noticeable variation in the oxide concentration during oscillations.[5,36,39] This means that the proposed mechanism has to be at least revised if not abandoned.

The comparison of the subsurface oxygen mechanism for Pd(110) with the surface phase transition model verified for Pt(100) and Pt(110)[2,3] reveals a common principle which has been realized in two different ways. Both mechanisms modify the catalytic activity via the change in the oxygen sticking coefficient. This is accomplished in the subsurface model by a chemical modification of the surface while structural changes modulate the oxygen sticking coefficient in the case of the surface phase transition model.[26–28] The different behavior of Pd and Pt surfaces can be traced back to their different tendency to form oxides. This tendency is much stronger for Pd. Despite this common principle an important difference remains between the two models. That is that a phase transition usually involves a sharp change of some properties at a certain critical coverage, while for the subsurface oxygen model the surface properties change continuously as the concentration of subsurface oxygen is var-

ied. This difference leads to differences in the bifurcation behavior as can be seen from a comparison with the three-variable model of the surface phase transition mechanism[28] or with the theoretical treatment of kinetic oscillations on Pt(100).[26,27] The question as to whether the two different models for kinetic oscillations are associated with qualitatively different bifurcation diagrams remains to be resolved by a detailed analysis of the subsurface oxygen model.

One of the topics which so far could not be reproduced by mathematical modeling is the occurrence of chaos in the catalytic CO oxidation. Low-dimensional chaos has been observed with kinetic oscillations on Pt(110) as demonstrated by a detailed analysis of the time series.[32] Related observations have been made with kinetic oscillations on Pd(110) although the appearance of deterministic chaos has not been proven by a detailed analysis of the data.[6,8] A clue what could be responsible for the complex dynamical behavior on Pd(110) was provided by the observation that chaos and period doubling on Pd(110) is found in the same parameter region where the bifurcation behavior becomes highly sensitive to very small parameter changes. With spatial inhomogeneities always being present, even on a well-prepared single crystal surface,[33] a pathway to chaos might exist via the gas phase coupling of surface areas with slightly different adsorption properties. Due to the narrowness of the bistable region spatial inhomogeneities can cause very strong coupling effects resulting in a complex dynamical behavior of the system. Formulated as a general principle chaos should then be possible on a parameter region where the bifurcation becomes sensitive enough to let spatial inhomogeneities of the catalyst come into play. Since it has been shown that thermal coupling of oscillating particles can cause chaotic behavior in the catalytic CO oxidation such a mechanism appears to be very promising.[34] Modeling of these kinds of effects is currently in progress for the present system.

V. CONCLUSIONS

Kinetic oscillations which occur in the catalytic CO oxidation on Pd(110) can be well described by a set of three coupled differential equations for the variations of the adsorbate coverages and the subsurface oxygen concentration. The mathematical model is based on reversible formation of subsurface oxygen whose presence decreases the catalytic activity as it lowers the oxygen sticking coefficient. During kinetic oscillations a periodic filling and depletion of the subsurface oxygen reservoir causes the surface reaction to switch between the two branches of the LH kinetics. The essential qualitative features of the experiment are well reproduced by this simple model: the reversal of the hysteresis in the reaction rate under oscillating conditions and the occurrence of kinetic oscillations in the vicinity of the rate maximum. The model also allows for a satisfactory fit of the existence region of kinetic oscillations and it reproduces most of the experimentally observed qualitative trends in the behavior of the oscillations. The bifurcation analysis shows the same type of transitions which have been observed in the experiment and it reproduces the increasing complexity of the dynamical behavior at low temperature. The mathematical modeling demonstrates that the simple subsurface oxygen model gives a reasonable description of kinetic oscillations in the system Pd(110)/CO + O_2.

ACKNOWLEDGMENTS

One of the authors (M. R. B.) was supported by the North Atlantic Treaty Organization under a grant awarded in 1988. The authors thank S. Wasle for the preparation of the drawings. They are indebted to H. Madden for carefully reading the manuscript and correcting the English and to M. Ehsasi for the permission to reproduce Fig. 4 of Ref. 6.

[1] L. F. Razón and R. A. Schmitz, Catal. Rev. Sci. Eng. **28**, 89 (1986).
[2] R. Imbihl, in *Optimal Structures in Heterogeneous Reaction Systems*, edited by P. J. Plath, Springer Series in Synergetics (Springer, Berlin, 1989).
[3] M. Eiswirth, P. Möller, K. Wetzl, R. Imbihl, and G. Ertl, J. Chem. Phys. **90**, 510 (1989).
[4] (a) J. E. Turner, B. C. Sales, and M. B. Maple, Surf. Sci. **103**, 54 (1981); (b) B. C. Sales, J. E. Turner, and M. B. Maple, *ibid.* **114**, 381 (1982).
[5] N. A. Collins, S. Sundaresan, and Y. J. Chabal, Surf. Sci. **180**, 136 (1987).
[6] M. Ehsasi, C. Seidel, H. Ruppender, W. Drachsel, J. H. Block, and K. Christmann, Surf. Sci. **210**, L198 (1989).
[7] S. Ladas, R. Imbihl, and G. Ertl, Surf. Sci. **219**, 88 (1989).
[8] M. Ehsasi, Thesis, University of Berlin (1989).
[9] (a) H. Niehus and G. Comsa, Surf. Sci. **93**, L147 (1980); (b) **102**, L14 (1981); (c) J. E. Turner and M. B. Maple, *ibid.* **147**, 647 (1984).
[10] T. Engel and G. Ertl, Adv. Catal. **28**, 1 (1979).
[11] G. Ertl and P. Rau, Surf. Sci. **15**, 443 (1969).
[12] J. Goschnick, M. Wolf, M. Grunze, W. N. Unertl, J. H. Block, and J. Loboda-Cacković, Surf. Sci. **178**, 831 (1986).
[13] J.-W. He and P. R. Norton, Surf. Sci. **204**, 26 (1988).
[14] J.-W. He, U. Memmert, K. Griffiths, and P. R. Norton, J. Chem. Phys. **90**, 5082 (1984).
[15] J.-W. He, U. Memmert, and P. R. Norton, J. Chem. Phys. **90**, 5088 (1989).
[16] M. Milun, P. Pervan, M. Vajić, and K. Wandelt, Surf. Sci. **211/212**, 887 (1989).
[17] J.-W. He, U. Memmert, K. Griffiths, W. N. Lennard, and P. R. Norton, Surf. Sci. **202**, L555 (1989).
[18] J. Goschnick, M. Grunze, J. Loboda-Cackovic, and J. H. Block, Surf. Sci. **189/190**, 137 (1987).
[19] J. Goschnick, J. Loboda-Cacković, J. H. Block, and M. Grunze in *Kinetics of Interface Reactions*, Springer Series in Surface Science (Springer, Berlin, 1987).
[20] T. Engel and G. Ertl, J. Chem. Phys. **69**, 1267 (1978).
[21] J.-W. He and P. R. Norton, J. Chem. Phys. **89**, 1170 (1988); see also for further references on Pd(110)/CO.
[22] J. Goschnick, Thesis, University of Berlin (1987).
[23] (a) G. Ertl and J. Koch, in *Adsorption–Desorption Phenomena*, edited by F. Ricca (Academic, London, 1972); (b) J. W. Park, Scr. Metall. **19**, 1481 (1985).
[24] P. Kisliuk, J. Phys. Chem. Solids **5**, 78 (1958).
[25] E. Doedel, 1981. AUTO: A program for the automatic bifurcation analysis of autonomous systems. Congressus Numerantium **30**: 265.
[26] R. Imbihl, M. P. Cox, G. Ertl, H. Müller, and W. Brenig, J. Chem. Phys. **83**, 1578 (1985).
[27] R. F. S. Andradé, G. Dewel, and P. Borckmans, J. Chem. Phys. **91**, 2675 (1989).
[28] K. Krischer, Thesis, University of Berlin (1990).
[29] R. Raval, S. Haq, M. A. Harrison, G. Blyholder, and D. A. King, Chem. Phys. Lett. **167**, 391 (1990).
[30] S. Ladas, R. Imbihl, and G. Ertl (in preparation).
[31] M. Eiswirth, K. Krischer, and G. Ertl, Appl. Phys. A (in press).
[32] M. Eiswirth, K. Krischer, and G. Ertl, Surf. Sci. **202**, 565 (1988).
[33] R. Imbihl, S. Ladas, and G. Ertl, Surf. Sci. **215**, L307 (1989).
[34] F. Schüth, X. Song, L. D. Schmidt, and E. Wicke, J. Chem. Phys. **92**, 745 (1990).
[35] B. C. Sales, J. E. Turner, and M. B. Maple, Surf. Sci. **112**, 272 (1981).
[36] R. C. Yeates, J. E. Turner, A. J. Gellman, and G. A. Somorjai, Surf. Sci. **149**, 175 (1985).
[37] H. Suhl, Surf. Sci. **107**, 88 (1981).
[38] E. P. Volokitin, S. A. Treskov, and G. S. Yablonskii, Surf. Sci. **169**, L321 (1986).
[39] F. Schüth and E. Wicke, Ber. Bunsenges. Phys. Chem. **93**, 191 (1989).